

A Spectroscopic Study of Kepler Asteroseismic Targets ¹

by

J. M o l e n d a - Ż a k o w i c z¹, A. F r a s c a², D.W. L a t h a m³ and M. J e r z y k i e w i c z¹

¹ Astronomical Institute, University of Wrocław, Kopernika 11,
51-622 Wrocław, Poland, e-mail: (molenda,mjertz)@astro.uni.wroc.pl

² Catania Astrophysical Observatory, Via S.Sofia 78,
95123 Catania, Italy, e-mail: afr@oact.inaf.it

³ Harvard-Smithsonian Center for Astrophysics, 60 Garden Street,
Cambridge, MA 02138, USA, e-mail: dlatham@cfa.harvard.edu

Received ...

ABSTRACT

Reported are spectroscopic observations of 15 candidates for Kepler primary asteroseismic targets and 14 other stars in the Kepler field, carried out at three observatories (see the footnote). For all these stars, the radial velocities, effective temperature, surface gravity, metallicity, and the projected rotational velocity are derived from two separate sets of data by means of two independent methods. In addition, MK type is estimated from one of these sets of data.

Three stars, HIP 94335, HIP 94734, and HIP 94743, are found to have variable radial-velocity. For HIP 94335 = FL Lyr, a well-known Algol-type eclipsing variable and a double-lined spectroscopic binary, the orbital elements computed from our data agree closely with those of Popper et al. For HIP 94734 and HIP 94743 = V 2077 Cyg, which we discover to be single-lined systems, orbital elements are derived. In addition, from our value of the orbital period and the Hipparcos epoch photometry, HIP 94743 is demonstrated to be a detached eclipsing binary.

Key words: *Space missions: Kepler – Stars : radial velocities – binaries: spectroscopic – binaries: eclipsing – Stars: atmospheric parameters – Stars: individual: FL Lyr, HIP 94734, V 2077 Cyg*

1. Introduction

Kepler² is a NASA space mission, scheduled for launch in February 2009. The Kepler equipment consists of a Schmidt telescope, with a 1.4-m primary mirror and a 0.95-m corrector plate, and a 430–890 nm FWHM bandpass photometer, featuring an array of 42 CCDs, 50×25 mm and 2200×1024 pixels each. The dynamic range is 9–15 mag. Kepler will observe pre-selected stars in a 12-degree field in the Cygnus-Lyra region. The same field will be observed for the entire life-time of the Kepler mission, i.e., at least 3.5 years. The main scientific goal is the detection of Earth-size and larger planets by means of the method of photometric transits (Borucki et al. 1997).

Kepler photometry will also be used for detecting solar-like pulsations in program stars and deriving accurate values of their pulsation frequencies, allowing an

¹Based in part on data obtained with the ESA Hipparcos satellite. The ground-based data used in this paper have been obtained at the *M.G. Fracastoro* station of the Catania Astrophysical Observatory, the Oak Ridge Observatory, Harvard, Massachusetts, and the F.L. Whipple Observatory, Mount Hopkins, Arizona.

²<http://kepler.nasa.gov/>

investigation of internal structure of these stars by means of asteroseismology (see, e.g., Christensen-Dalsgaard 2004). This investigation will be carried out by members of KASC³ under the lead of J. Christensen-Dalsgaard from the Department of Physics and Astronomy of the Aarhus University.

Molenda-Żakowicz et al. (2006) have provided a list of 104 Hipparcos stars that were selected as candidates for asteroseismic targets for Kepler. These authors list 29 candidates for primary asteroseismic targets, one being a binary whose components are treated separately by Molenda-Żakowicz et al. (2006) but as an individual object in this paper. Since 14 of these stars fall either just beyond the Kepler CCD chips or into star tracker corners, and are not expected to be observed in normal conditions, in the present paper we narrow down the definition of the primary asteroseismic targets (hereafter, PATS) to 15 stars that fall onto active chips of Kepler CCDs.

We expect all these stars to show solar-like oscillations with amplitudes possible to be detected in Kepler photometry. Having the oscillation frequencies measured, the internal structure of these objects will be examined by means of the asteroseismic analysis. The results of this study, particularly the values of the stellar radii, will be used by the Kepler team for determining the radii of planets and the parameters of the planetary systems, providing that such will be discovered.

Since the model computations require the effective temperature, surface gravity, metallicity, and the projected rotational velocity to be input parameters, in 2005 we started a program of ground-based observations, aiming at the determination of these parameters. In this paper, we present the results of our spectroscopic study, obtained for all the 29 stars.

After giving an account of the spectroscopic observations and reductions in Sect. 2, in Sect. 3 we discuss three stars showing variable radial velocity, one known Algol-type eclipsing variable and a double-lined spectroscopic binary, HIP 94335 = FL Lyr, and two single-lined spectroscopic binaries, HIP 94734 and HIP 94743 = V 2077 Cyg, discovered in the present work. For HIP 94335 we find the orbital elements computed in this paper to be in a very good agreement with those of Popper et al. (1986). For HIP 94734 and HIP 94743, we derive orbital elements for the first time. In addition, using our value of the orbital period and the Hipparcos epoch photometry (ESA 1977), we demonstrate that HIP 94743 is a detached eclipsing binary. In Sect. 4, we determine the effective temperature, surface gravity, metallicity, and MK spectral type of the 29 stars; in Sect. 5, we give their projected rotational velocity. Sect. 6 contains a summary.

2. Observations and Reductions

The observations were carried out at the *M.G. Fracastoro* station (Serra La Nave, Mount Etna, elevation 1750 m) of the Catania Astrophysical Observatory (CAO), Italy (74 spectrograms), at the Oak Ridge Observatory (ORO), Harvard, Massachusetts (32 spectrograms), and at the F.L. Whipple Observatory (FLWO), Mount Hopkins, Arizona (126 spectrograms).

At CAO, we used a 91-cm telescope and the fiber-fed echelle spectrograph FRESKO. The spectra were recorded with resolving power $R=21\,000$ in a wide spectral range that covered about $2\,500\text{ \AA}$ in 19 orders. As the detector, we used a thinned back-illuminated CCD SITE chip (SI033B) with $1024\times 1024\text{ }24\times 24\text{-}\mu\text{m}$

³<http://astro.phys.au.dk/KASC/> Kepler Asteroseismic Science Consortium (KASC) is an international consortium of researchers dedicated to the asteroseismic analysis of Kepler data. It is a part of the Kepler Asteroseismic Investigation, which is coordinated by the Department of Physics and Astronomy, University of Aarhus, Denmark.

T a b l e 1

15 G-type dwarfs used for calculating the offset between radial velocities measured with FRESCO, R.V.(F), and those measured with the CfA Speedometers, R.V.(CfA). The last three columns contain the number and time-span of observations made with the CfA Speedometers, N_{CfA} and Span (CfA), and the difference between the R.V. values measured with FRESCO and the CfA Speedometers, $\Delta\text{R.V.} = \text{R.V.}(F) - \text{R.V.}(CfA)$

HD	R.V.(F)	s.e.	R.V.(CfA)	s.e.	N_{CfA}	Span (CfA)	$\Delta\text{R.V.}$
90839	+10.13	0.25	+8.39	0.46	67	9900	+1.74
99984	-32.26	0.33	-33.00	0.48	18	9883	+0.74
102870	+5.13	0.24	+4.25	0.46	298	10072	+0.88
107213	-9.56	0.37	-9.61	0.56	32	7945	+0.05
114710	+6.58	0.22	+5.22	0.52	150	9048	+1.36
123782	-15.14	0.25	-14.12	0.76	33	5967	-1.02
136064	-48.12	0.30	-48.44	0.44	17	9207	+0.32
142373	-56.10	0.27	-56.39	0.44	41	10303	+0.29
161096	-11.91	0.12	-12.32	0.44	113	5596	+0.41
185144	26.04	0.22	+26.05	0.47	6	2983	-0.01
186408	-28.07	0.25	-27.38	0.44	16	5141	-0.69
186427	-27.79	0.16	-28.13	0.53	23	7122	+0.34
187691	+0.55	0.24	-0.15	0.40	517	9269	+0.70
201891	-44.68	0.26	-44.78	0.56	25	6694	+0.10
219623	-25.97	0.25	-27.29	0.49	15	8897	+1.32

pixels.

The telescope used at ORO was the 1.5-m Wyeth reflector. At FLWO, two telescopes were used, viz., the 1.5-m Tillinghast reflector and the Multiple Mirror Telescope (before it was converted to the monolithic 6.5-m mirror). The spectra were obtained by means of echelle spectrographs with resolving power $R=35\,000$ (CfA Digital Speedometers). The detector consisted of an intensified photon-counting Reticon. In this system, a single 45 \AA spectrogram, centered at $\lambda \simeq 5187\text{ \AA}$, was recorded in one exposure.

The spectrograms measured with FRESCO were reduced with the use of IRAF⁴. The spectra were extracted with the `apall` task and the radial velocities were determined *via* the cross-correlation method, also provided by IRAF in the `fxcor` task. Arcturus, β Oph, 54 Aql, 31 Aql or γ Aql, for which precise values of R.V. are available (Udry et al. 1999), served as the radial-velocity templates. These stars were observed on the same nights as the program stars. Care was taken to match spectral types of the template and program star as closely as possible.

Spectra measured at ORO and FLWO were extracted and rectified by means of a special procedure developed for these observatories and described in detail in Latham et al. (1992). For the templates, the grid of synthetic spectra, based on model atmospheres of R.L. Kurucz and computed by Jon Morse for this specific wavelength window and resolution was used (see Torres et al. 2002).

Before the analysis of radial velocities was started, all measurements were moved to one reference system. We calculated the offset in radial velocity using the mean values of R.V. measured for 15 G-type dwarfs with FRESCO (single measurements,

⁴IRAF is distributed by the National Optical Astronomy Observatory, which is operated by the Association of Universities for Research in Astronomy, Inc.

T a b l e 2

Radial velocities (in km/s) of the program stars.
 The code in the last column indicate stars that fall onto the active chips of Kepler CCDs, “A”, stars that fall into CCD gaps, “G”, or stars that fall into star tracker corners, “S”.
 The individual velocities are not corrected for the shift between observatories

HIP	HJD-2400000	R.V.	s.e.	Instrument	code
91128	45839.7031	-31.43	0.54	Wyeth	S
91128	45839.9676	-32.04	0.39	Tillinghast	S
91128	53512.8557	-32.15	0.37	Tillinghast	S
91128	53517.8486	-32.05	0.36	Tillinghast	S
91128	53894.3541	-31.47	0.56	FRESCO	S
92922	51784.6670	-39.68	0.71	Wyeth	G
92922	53512.8595	-40.03	0.26	Tillinghast	G
92922	53517.8522	-39.82	0.35	Tillinghast	G
92922	53549.3790	-39.00	0.23	FRESCO	G
92922	53555.4006	-38.58	0.19	FRESCO	G
93011	53512.8629	-23.43	0.90	Tillinghast	A
93011	53517.8551	-23.69	0.88	Tillinghast	A
93011	53552.3660	-21.74	0.92	FRESCO	A
93011	53558.5257	-21.62	0.71	FRESCO	A
94145	53512.8669	0.76	0.40	Tillinghast	G
94145	53517.8586	3.41	0.49	Tillinghast	G
94145	53543.9805	1.32	0.53	Tillinghast	G
94145	53549.4241	2.25	0.24	FRESCO	G
94145	53553.5995	3.04	0.29	FRESCO	G
94145	53659.6048	3.56	0.63	Tillinghast	G
94145	53895.3536	2.23	0.72	FRESCO	G
.....
99267	53905.4480	-193.98	1.65	FRESCO	S

mean values over 19 orders) and the CfA Digital Speedometers (long time-span of observations and tens or hundreds measurements). In Table 1, we list these 15 stars, their mean radial velocity in km s^{-1} measured with FRESCO and CfA Speedometers, the standard deviation of the measurements, the number of CfA Speedometers’ spectrograms, N_{CfA} , the time-span of CfA observations in days, and the difference between the mean radial velocity values. We conclude that the FRESCO zero-point is stable in time, which allows us to combine the data sets, and that the unweighted average difference between the FRESCO and CfA zero-point is equal to $+0.44 \pm 0.19$. With this in mind, we merged the FRESCO and CfA Digital Speedometers’ observations, subtracting 0.5 km s^{-1} from each FRESCO’s measurement. All results that we discuss in this paper are obtained from the merged data.

In Table 2, we give the individual radial-velocity measurements not corrected for this offset. The table is available in electronic form from the Acta Astronomica Archive (see the cover page). A sample, containing the heading, the first 21 rows, and the last row, is printed below. In the first column we give the HIP number,

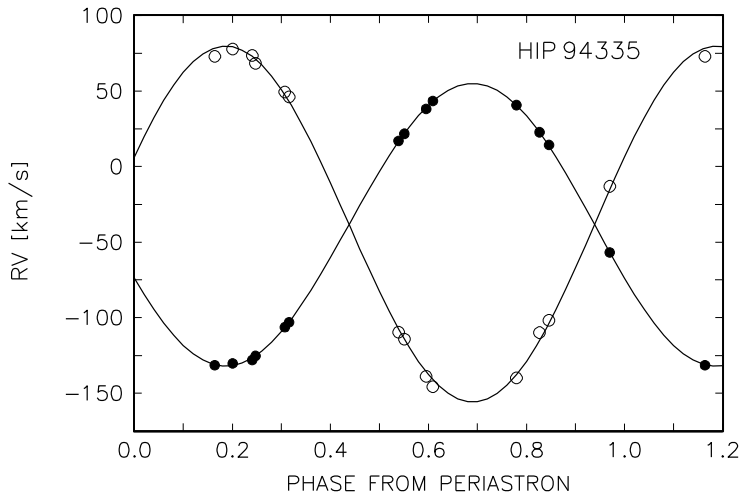


Figure 1: The radial-velocity observations of HIP 94335 = FL Lyr from Table 2 corrected for the shift between observatories. The radial-velocities of the primary component are shown with filled circles, and those of the secondary component, with open circles. The lines represent the orbital solution given in Table 4.

in the second, the Heliocentric Julian Day of the middle of the exposure, in the third and fourth, the radial velocity, R.V., and the standard error, s.e., then, the instrument used, and in the last column, the information whether the star falls onto the active pixels of Kepler CCDs, coded with “A”, into the gaps between CCD chips, coded with “G”, or into a star tracker corner, coded with “S”.

In Table 3, we list the 15 PATS and the 14 remaining stars, their mean radial velocity, R.V., in km s^{-1} , the ratio of external-to-internal error, e/i , the sum of the residuals divided by the internal error estimate squared, χ^2 , and the probability that a star with constant velocity will have χ^2 values larger than the observed one, $P(\chi^2)$, or, for the double stars, the classification to the type of spectroscopic binarity. For detailed description of the method of computing the respective errors, we refer to Latham et al. (2002).

3. Program Stars with Variable Radial-Velocity

3.1. HIP 94335 = FL Lyr

In Table 2, there are 14 R.V. measurements of FL Lyr per component, twelve Tillinghast and two FRESCO. In the table, the primary component is denoted HIP 94335-1, and the secondary component is denoted HIP 93335-2. An orbital solution, obtained from the merged data (corrected for the offset between our observatories), with equal weights assigned to all measurements, is listed in Table 4. A phase diagram, computed using this solution, is shown in Fig. 1.

A comparison of the numbers from Table 4 with the orbital elements of FL Lyr given in Table XVI of Popper et al. (1986) shows that (1) the two solutions are of similar accuracy, and (2) in no case the difference between the corresponding elements exceeds one standard deviation.

There is also a very good agreement between the value of the orbital period given by Popper et al. (1986) in their Table VII and the value obtained by dividing the difference of the epoch of our R.V. changing from recession to approach and their epoch of the primary (photometric) minimum by the number of cycles that had elapsed between the two epochs. The difference between these two values of

T a b l e 3

15 PATS and the remaining 14 stars: mean radial velocity, R.V., in km s^{-1} , the ratio of external-to-internal error, e/i, the sum of the residuals divided by the internal error estimate squared, χ^2 , and the probability that a star with constant velocity will have χ^2 values larger than the observed one, $P(\chi^2)$, or the classification to the type of spectroscopic variability

HIP	α_{2000}	δ_{2000}	N	span	R.V.	s.e.	e/i	χ^2	$P(\chi^2)$
PATS									
93011	18 56 53.36	+48 41 38.4	4	46	-22.87	0.44	0.9	2.6	0.46
94335	19 12 04.86	+46 19 26.5	14	181	-38.32	0.25	58.7	3293.6	SB2
94497	19 13 58.83	+39 50 37.4	5	1772	+7.64	0.19	0.8	2.6	0.63
94565	19 14 45.00	+51 08 42.4	6	916	-10.82	0.20	1.1	2.8	0.42
94734	19 16 34.89	+40 02 48.8	16	916	-25.46	1.01	7.0	50.2	SB1
95098	19 20 47.91	+44 09 18.7	5	916	+10.41	0.19	0.4	0.4	0.94
95637	19 27 13.74	+50 50 56.5	4	46	-11.61	0.40	0.7	1.7	0.65
95733	19 28 21.01	+39 04 50.6	5	917	+20.52	0.35	0.6	1.6	0.79
96634	19 38 51.16	+43 52 28.2	5	1769	+15.25	0.27	0.4	1.2	0.88
96735	19 39 52.12	+45 09 33.0	5	1299	-16.64	0.19	0.6	1.4	0.85
97219	19 45 30.09	+50 46 18.8	12	4331	-20.65	0.16	1.1	12.8	0.31
97337	19 47 10.19	+40 20 25.0	1	0	-70.50	0.49	0.0	0.0	1.00
97657	19 50 50.14	+48 04 49.1	7	1996	-63.55	0.15	0.8	4.6	0.60
97974	19 54 41.18	+42 25 50.5	2	47	-31.75	0.34	0.9	0.7	0.39
98655	20 02 17.06	+45 46 58.0	4	396	-52.20	0.28	1.2	4.6	0.20
The remaining stars									
91128	18 35 18.01	+45 44 35.4	5	8055	-31.93	0.23	0.6	1.1	0.90
92922	18 55 54.82	+41 31 17.7	5	1771	-39.62	0.20	0.8	4.6	0.33
94145	19 09 49.51	+44 33 26.9	8	386	+2.36	0.40	1.8	26.8	0.00
94704	19 16 13.40	+37 04 18.8	4	2031	-347.30	0.39	0.6	0.9	0.83
94743	19 16 44.50	+50 38 47.8	30	917	-0.40	0.66	24.7	750.8	SB1
94898	19 18 41.45	+43 14 12.5	6	2122	-37.34	0.38	2.1	22.6	0.00
95631	19 27 05.78	+46 27 14.5	6	1771	-24.34	0.20	1.0	9.7	0.08
95638	19 27 14.11	+43 15 38.5	3	391	-32.04	0.54	2.0	7.4	0.03
95843	19 29 35.34	+45 30 46.3	4	40	-22.02	0.27	0.8	1.6	0.67
96146	19 32 56.38	+50 55 52.1	4	43	-29.45	0.72	1.8	10.0	0.02
97168	19 44 59.23	+51 35 41.1	5	1679	-91.65	0.29	1.3	6.5	0.16
98381	19 59 19.33	+42 10 06.4	5	1772	-73.14	0.24	1.1	4.2	0.38
98829	20 04 10.58	+42 30 43.6	6	2574	-42.01	1.13	5.9	133.1	0.00
99267	20 09 01.32	+42 51 52.0	46	8425	-196.10	0.14	1.3	76.6	0.00

T a b l e 4

Orbital elements of HIP 94335 = FL Lyr

$$\begin{aligned}
P_{\text{orb}} &= 2.178097 \pm 0.000058 \text{ d} \\
\gamma &= -38.36 \pm 0.27 \text{ km s}^{-1} \\
K_1 &= 93.54 \pm 0.34 \text{ km s}^{-1} \\
K_2 &= 117.71 \pm 1.21 \text{ km s}^{-1} \\
e &= 0.0063 \pm 0.0037 \\
\omega_1 &= 112^\circ \pm 47^\circ \\
T &= \text{HJD } 2453595.10 \pm 0.28 \\
a_1 \sin i &= (2.802 \pm 0.010) \times 10^6 \text{ km} \\
a_2 \sin i &= (3.525 \pm 0.036) \times 10^6 \text{ km} \\
M_1 \sin^3 i &= 1.190 \pm 0.020 M_\odot \\
M_2 \sin^3 i &= 0.944 \pm 0.012 M_\odot
\end{aligned}$$

T a b l e 5

Orbital elements of HIP 94734

$$\begin{aligned}
P_{\text{orb}} &= 98.92 \pm 0.17 \text{ d} \\
\gamma &= -25.47 \pm 0.45 \text{ km s}^{-1} \\
K_1 &= 16.18 \pm 0.75 \text{ km s}^{-1} \\
e &= 0.195 \pm 0.025 \\
\omega_1 &= 132.^\circ 3 \pm 9.^\circ 9 \\
T &= \text{HJD } 2454008.8 \pm 2.6 \\
a_1 \sin i &= (2.16 \pm 0.10) \times 10^7 \text{ km} \\
f(M) &= 0.0410 \pm 0.0057 M_\odot
\end{aligned}$$

the orbital period amounts to $(6 \pm 5) \times 10^{-7}$ d.

3.2. HIP 94734

For this star we have 16 measurements (see Table 2). The highest peak in the periodogram of these data occurs near 0.01 c/d. We conclude that HIP 94734 is an SB1 system with orbital period close to 100 d. Assigning equal weights to all points, we derived the orbital elements given in Table 5. A phase diagram, computed using these elements is shown in Fig. 2.

3.3. HIP 94743 = V 2077 Cyg

This star was classified as a suspected eclipsing binary, E:, by Kazarovets et al. (1999) on the basis of Hipparcos photometry (ESA 1997). However, no period is reported in the Hipparcos catalogue. A periodogram of our 29 radial-velocity observations of the star (see Table 2) is dominated by a peak at 0.1684 d^{-1} . A sine-curve of this frequency fits the data satisfactorily. We conclude that HIP 94743 is an SB1 system with orbital period close to 5.938 d and small eccentricity. Assigning equal weights to all points, we derived the orbital elements given in Table 6. A phase diagram, computed using these elements, is shown in Fig. 3.

Hipparcos magnitudes of the star phased with $P_{\text{orb}} = 5.93733$ d show two minima

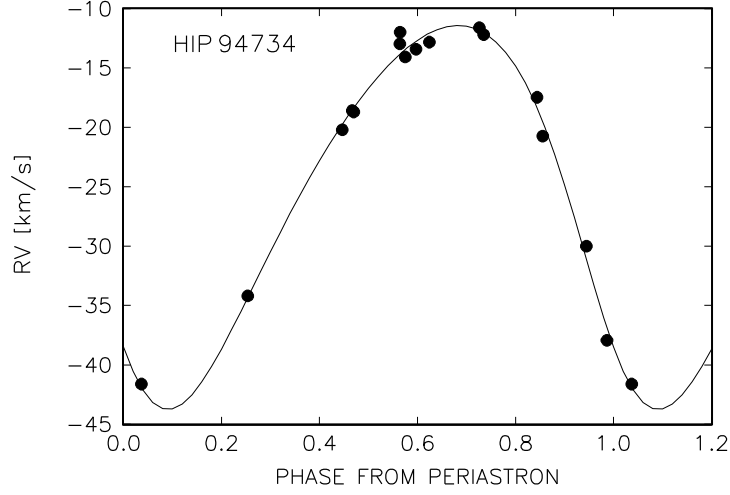


Figure 2: The radial-velocity observations of HIP 94734 from Table 2 corrected for the shift between observatories (circles). The line represents the orbital solution given in Table 5.

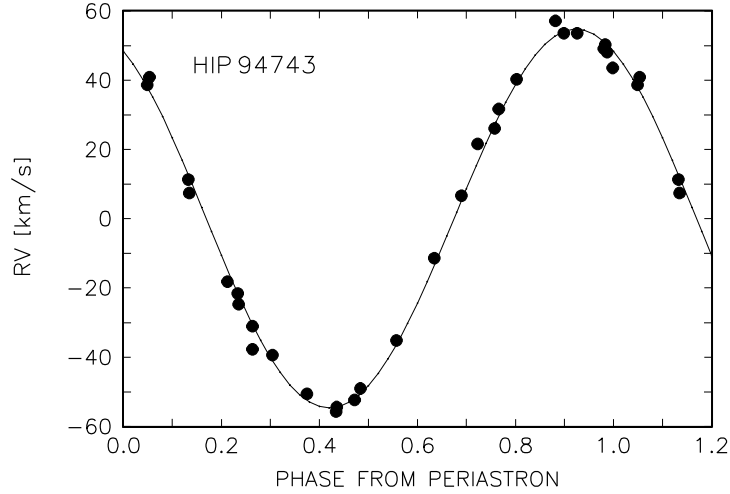


Figure 3: The radial-velocity curve of HIP 94743 = V 2077 Cyg from Table 2 corrected for the shift between observatories (circles). The line represents the orbital solution given in Table 6.

T a b l e 6

Orbital elements of HIP 94743 = V 2077 Cyg

$$\begin{aligned}
 P_{\text{orb}} &= 5.93733 \pm 0.00025 \text{ d} \\
 \gamma &= -0.42 \pm 0.54 \text{ km s}^{-1} \\
 K_1 &= 54.73 \pm 0.69 \text{ km s}^{-1} \\
 e &= 0.010 \pm 0.012 \\
 \omega_1 &= 28^\circ \pm 87^\circ \\
 T &= \text{HJD } 2453952.7 \pm 1.4 \\
 a_1 \sin i &= (4.468 \pm 0.056) \times 10^6 \text{ km} \\
 f(M) &= 0.1011 \pm 0.0038 M_\odot
 \end{aligned}$$

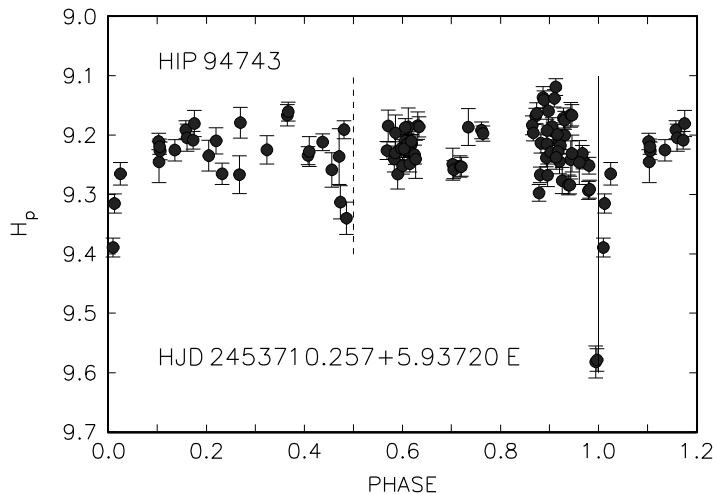


Figure 4: The Hip magnitudes of HIP 94743 = V 2077 Cyg (circles with error bars). The phases were computed with the ephemeris shown. Phases 0 and 0.5 are indicated by the solid and dashed vertical line, respectively.

of unequal depths, separated in phase by 0.5. The epoch of the primary minimum is shifted from the epoch of our R.V. changing from recession to approach by 0.06 in phase. Taking into account the fact that some 885 cycles have elapsed between the mid-epochs of the Hipparcos and our data, we get a slightly improved value of the orbital period, $P_{\text{orb}} = 5.93720 \pm 0.00013$ d. The Hip magnitudes of HIP 94743 are plotted as a function of phase of this period in Fig. 4. As can be seen from the figure, the system is widely detached.

3.4. Two Unconfirmed Spectroscopic Binaries

Of the remaining stars, HIP 97219 = HD 187055 was reported to be variable in radial velocity by Nordström et al. (2004), and HIP 99267 = G125-64 was suspected to be a spectroscopic binary by Carney & Latham (1987). Nordström et al. (2004) based their conclusion on four Coravel measurements. Our 12 radial-velocities of HIP 97219 include eight Wyeth measurements. As can be seen from Table 2, the (external) standard deviation of the latter data and the mean value of their s.e. are both equal to 0.5 km s^{-1} . In addition, the remaining measurements (three Tillinghast and one FRESCO) fall within the range of 1.6 km s^{-1} defined by the Wyeth data. Clearly, the star's R.V. does not vary by more than 1.6 km s^{-1} . The $P(\chi^2)$ computed from our observations is equal to 0.3 and the ratio of external-to-internal error is equal to 1.1. Thus, we do not confirm the result of Nordström et al. (2004). However, our data may not exclude the case of a very eccentric orbit for which we covered only the flat portion of the R.V. curve.

For HIP 99267 = G125-64 there are 46 R.V. measurements in Table 2. These data include 19 discovery observations of Carney & Latham (1987). The time distribution of the data is not uniform: after the first 42 measurements, which cover an interval of eight years, there is a gap of almost 14 years; the last four measurements span an interval of one year. Disregarding these four measurements, one gets a range of 5.3 km s^{-1} and a standard deviation of 1.1 km s^{-1} . Comparing the latter value with the s.e. (which range from 0.9 to 1.7 km s^{-1}) we conclude that better data are needed to confirm the binary status of the star. We note also that the above-mentioned range of 5.3 km s^{-1} is defined by measurements with the

second and third largest s.e. and that although the $P(\chi^2)$ computed from our data is equal to zero, the ratio of external-to-internal error is equal to 1.3 only.

4. Effective Temperature, Surface Gravity, Metallicity, and the MK Type

4.1. From a Comparison with Standard Stars

We have determined T_{eff} , $\log g$ and $[\text{Fe}/\text{H}]$ of the program stars from the FRESCO spectrograms using ROTFIT, an IDL code developed by A.F. and his coworkers (see, e.g., Frasca et al. 2003, 2006). The method used by ROTFIT is similar to that of Katz et al. (1998) and Soubiran et al. (1998). It consists in comparing the spectra of program stars with a library of spectra of reference stars. The aim is to find 10 reference stars that best reproduce the target spectrum. The weighted means of their astrophysical parameters, T_{eff} , $\log g$, and $[\text{Fe}/\text{H}]$, are adopted as estimates of the astrophysical parameters of the program star. The spectrograms have to be cleaned of instrumental effects and cosmic rays, and brought to the same spectral resolution, the same wavelength scale and the same continuum level. The spectrogram of each program star is compared order by order with the spectrograms of the reference stars by the method of least squares. Since the reference and the program stars may have different rotational velocities, in the process of comparison the reference spectra are broadened in a wide range of $v \sin i$ to find the best match. The value of χ^2 is used as a measure of the similarity of spectra.

As discussed by Katz et al. (1998), Soubiran et al. (1998), and Frasca et al. (2006), this method allows simultaneous and fast determination of T_{eff} , $\log g$, and $[\text{Fe}/\text{H}]$ even from spectrograms of low signal-to-noise ratio (S/N) or moderate resolution. This is a clear advantage over the classical methods, based on fitting specific lines or spectral regions with synthetic spectra, that normally require spectrograms of high resolution and high S/N. Moreover, classical methods require *a priori* information on T_{eff} and $\log g$ to determine $[\text{Fe}/\text{H}]$ because this parameter depends on the two others.

In order to adopt this method to our purpose we have compiled a list of 240 slowly rotating reference stars ($v \sin i < 15 \text{ km s}^{-1}$) for which spectrograms are available from the ELODIE archive (Prugniel & Soubiran 2001). This archive contains high-resolution ($R = 42\,000$) and high S/N spectrograms obtained with the Haute-Provence Observatory's 193-cm telescope and the fiber-fed echelle spectrograph ELODIE. For the majority of our reference stars, we adopted T_{eff} , $\log g$, and $[\text{Fe}/\text{H}]$ from the TGMET library of Soubiran et al. (1998). For stars that are not included in this library, we adopted recent values of T_{eff} , $\log g$, and $[\text{Fe}/\text{H}]$ from the literature. In Table 7, available electronically from the Acta Astronomica archive, we list the 240 stars and their T_{eff} , $\log g$, and $[\text{Fe}/\text{H}]$. For stars that are not included in the TGMET library, the references are given at the bottom of the table. As can be seen from the table, the values of T_{eff} , $\log g$, and $[\text{Fe}/\text{H}]$ of our ELODIE reference stars are in the ranges [3700 K, 10800 K], [0.2, 4.9], and [0.50, -2.38], respectively, wide enough to cover the expected ranges of the parameters of program stars. The last column of Table 7 contains the MK spectral type, compiled from the literature, with the Hipparcos Input Catalogue used as a guide.

Since the ELODIE reference stars and the program stars were observed with different instruments and different resolutions, in the analysis we had to degrade the ELODIE spectrograms to match the lower resolution of FRESCO. To check whether this procedure affects the resulting atmospheric parameters, we performed parallel computations with ROTFIT using reference stars observed with FRESCO.

In order to save the observing time, we have chosen a less dense grid of slowly rotating reference stars with known astrophysical parameters. The list contains only 82 stars with T_{eff} , $\log g$, and $[\text{Fe}/\text{H}]$ in the ranges [3300 K, 7700 K], [0.70, 4.55], and [0.35, -2.65], respectively. Since the grid is coarse close to its edges, we have determined the atmospheric parameters only for these stars that fall into the ranges [4750 K, 6750 K], [3.8, 4.6], and [-0.5, 0.5] for $\log T_{\text{eff}}$, $\log g$, and $[\text{Fe}/\text{H}]$, respectively, where the grid is dense enough to make our determinations reliable. In Table 8, available electronically from the Acta Astronomica Archive, we list the FRESCO reference stars and their adopted atmospheric parameters. As before, for the majority of stars we used the values from the TGMET library of Soubiran et al. (1998), and for the remaining stars we adopted recent determinations from the literature, referenced at the bottom of the table.

For each program star, we have selected five most similar ELODIE reference stars from Table 7 (those giving the lowest χ^2 values) and computed means of their T_{eff} , $\log g$, and $[\text{Fe}/\text{H}]$. The resulting values we consider to be representative for the program stars. They are listed in Table 9. In the last but one column of the table, we give MK spectral type assigned using a mean of MK types of two most similar reference stars selected in each order. We find our classification fully consistent with the relations between T_{eff} and spectral type given by Johnson (1966) for dwarfs and giants. For metal-deficient program stars no comparison was possible because Johnson (1966) does not consider such stars. In the last column of Table 9, we list spectral types taken from the Simbad database.

In addition, for 16 program stars that fall within the limits of the FRESCO grid we derived means of T_{eff} , $\log g$, and $[\text{Fe}/\text{H}]$ using reference stars from Table 8. In this case, we used three most similar reference stars for each program star. The results are given in Table 10.

In Fig. 5 (left panels), we show the ELODIE reference stars and the program stars, plotted in three two-parameter planes, viz., $T_{\text{eff}} - \log g$, $T_{\text{eff}} - [\text{Fe}/\text{H}]$, and $\log g - [\text{Fe}/\text{H}]$. For clarity, the diagrams are zoomed to regions occupied by the program stars, so that the reference stars falling outside the panels are not shown.

The right panels of Fig. 5 show the FRESCO reference stars (see Table 8) and program stars from Table 10. In this figure, the ranges of the parameters are those that we have used for computing the astrophysical parameters of program stars.

All 16 stars from Table 10 appear also in Table 9. For these stars, the difference between the ELODIE and FRESCO based values of the effective temperature, $T_{\text{eff}}(\text{ELODIE}) - T_{\text{eff}}(\text{FRESCO})$, is plotted as a function of $T_{\text{eff}}(\text{ELODIE})$ in the upper left panel of Fig. 6. The values agree well to within the error bars. The largest discrepancy, amounting to about 400 K, occurs for HIP 95733. If we reject this star, we find the mean difference between T_{eff} determined from these two grids to be equal to -27 ± 28 K. The cause of the discrepancy in case of HIP 95733 is unclear.

For $\log g$, the difference $\log g(\text{ELODIE}) - \log g(\text{FRESCO})$ is shown in the left middle panel. As can be seen from the figure, the $\log g$ values show adequate agreement, although the values based the FRESCO grid are systematically – albeit slightly – larger than those based on the ELODIE grid. The mean difference between $\log g$ determined from these two grids is equal to -0.03 ± 0.03 dex.

The ELODIE and FRESCO values of $[\text{Fe}/\text{H}]$ are compared in the bottom panel of Fig. 6. All points agree well; the mean difference between $[\text{Fe}/\text{H}]$ determined from these two grids is equal to -0.04 ± 0.07 dex.

We conclude that both grids, ELODIE and FRESCO, can be safely used for our purpose. The ELODIE grid, however, is more useful at this stage because it is sufficiently wide and dense, allowing a better determination of astrophysical parameters for stars falling in the coarse parts of the FRESCO grid.

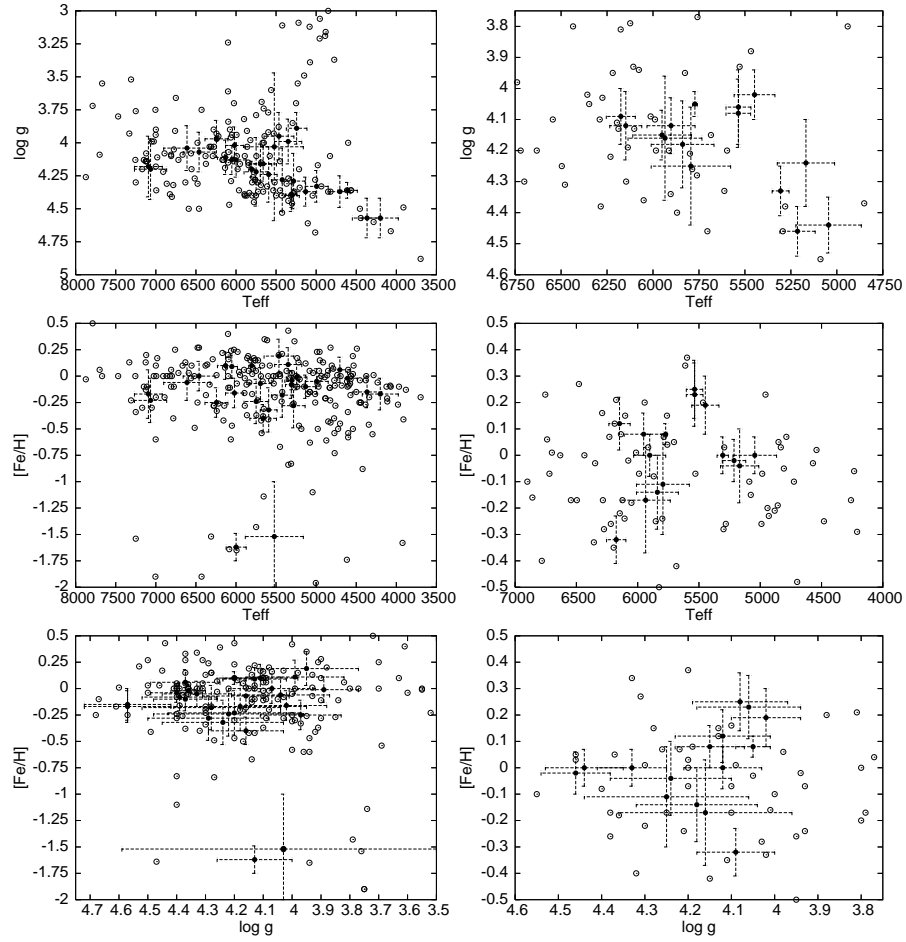


Figure 5: *Left:* Distribution of the ELODIE reference stars from Table 7 (open circles) and the program stars from Table 9 (filled circles) in the $T_{\text{eff}}-\log g$, $T_{\text{eff}}-[\text{Fe}/\text{H}]$ and $\log g-[\text{Fe}/\text{H}]$ planes. *Right:* The same for FRESCO reference stars from Table 8 (open circles) and program stars from Table 10 (filled circles). For clarity, the diagrams are zoomed to the regions occupied by the program stars.

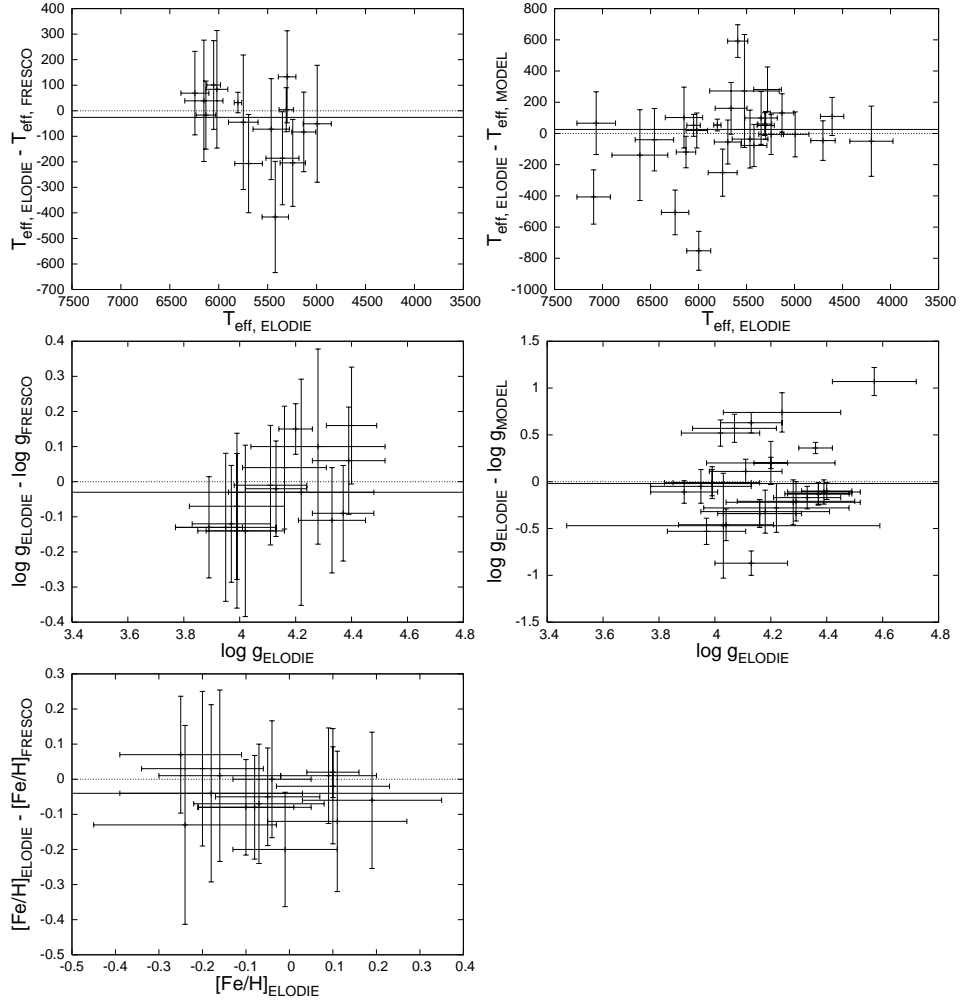


Figure 6: Differences, $T_{\text{eff}}(\text{ELODIE}) - T_{\text{eff}}(\text{FRESCO})$ (upper left panel), $\log g(\text{ELODIE}) - \log g(\text{FRESCO})$ (middle left panel), and $[\text{Fe}/\text{H}]$ (bottom left panel), between ELODIE and FRESCO determinations, and respective differences between ELODIE and model determinations plotted for T_{eff} (upper right panel) and $\log g$ (lower right panel). The dashed lines are zero lines; the solid lines show the mean difference between the computed values.

T a b l e 9

Astrophysical parameters and MK spectral types of PATS and the remaining stars determined with the use of the ELODIE library. In the last column, we list spectral types from the literature

HIP	T_{eff}	s.d.	$\log g$	s.d.	[Fe/H]	s.d.	MK	lit.
PATS								
93011	6460	200	4.07	0.15	0.00	0.14	F5IV	F2
94335	6152	195	3.99	0.14	-0.20	0.14	F8V	F8V+G8V
94497	4994	144	4.33	0.12	-0.05	0.12	K2V	K2
94565	6052	70	4.13	0.11	0.09	0.11	G0IV	G0
94734	5804	38	4.20	0.06	0.10	0.06	G2V	—
95098	6019	112	4.02	0.14	-0.16	0.14	F8III-IV	F8
95733	5423	135	4.28	0.24	-0.18	0.21	G8V	—
95637	6611	291	4.04	0.17	-0.06	0.17	F2III	F0
96634	5310	73	4.39	0.13	-0.08	0.13	K0V	K0
96735	5131	123	4.37	0.11	-0.10	0.11	K2V	K0
97219	5301	90	4.40	0.09	-0.04	0.09	K0V	G5
97337	4365	184	4.57	0.15	-0.15	0.15	K7V	M0
97657	4704	127	4.37	0.12	0.06	0.12	K3V	K2
97974	5749	151	4.22	0.26	-0.24	0.21	G0V	G0
98655	5282	144	4.29	0.21	-0.28	0.21	G9V	K0
The remaining stars								
91128	4200	225	4.57	0.15	-0.17	0.15	K7V	M0
92922	5464	186	3.95	0.18	0.19	0.16	G8IV	G5
94145	7093	174	4.18	0.23	-0.17	0.23	F0III	F0III
94704	5522	362	4.03	0.56	-1.52	0.52	sdG0	K2
94743	7066	201	4.20	0.23	-0.23	0.21	F2V	F5
94898	5244	129	3.89	0.12	-0.01	0.12	G8IV	G5
95631	5349	169	3.99	0.17	0.11	0.16	G9IV	G5
95638	5695	141	4.16	0.15	-0.07	0.15	G5V	G5
95843	6244	143	3.97	0.14	-0.25	0.14	F2V	F2
96146	6131	101	4.11	0.13	0.10	0.13	F8IV-V	F0
97168	5661	166	4.16	0.13	-0.40	0.13	G0V	—
98381	4609	122	4.36	0.06	-0.02	0.06	K4V	K2
98829	5592	105	4.24	0.21	-0.32	0.21	G8V	G5
99267	5998	125	4.13	0.13	-1.62	0.13	sdF2	F3

T a b l e 10
 Astrophysical parameters of 10 PATS and six remaining stars determined with the
 use of the FRESKO library

HIP	T_{eff}	s.d.	$\log g$	s.d.	[Fe/H]	s.d.
PATS						
94335	6113	136	4.13	0.17	-0.23	0.17
94497	5045	178	4.44	0.09	0.00	0.07
94565	5951	159	4.15	0.08	0.08	0.08
94734	5772	13	4.05	0.04	0.08	0.04
95098	5935	201	4.16	0.20	-0.17	0.20
95733	5839	171	4.18	0.14	-0.14	0.14
96634	5306	46	4.33	0.08	0.00	0.07
96735	5214	96	4.46	0.08	-0.02	0.08
97219	5168	156	4.24	0.14	-0.04	0.14
97974	5794	216	4.25	0.19	-0.11	0.19
The remaining stars						
92922	5536	67	4.08	0.11	0.25	0.11
94898	5448	111	4.02	0.08	0.19	0.11
95631	5535	68	4.06	0.12	0.23	0.12
95638	5902	131	4.12	0.09	0.00	0.08
95843	6175	79	4.09	0.09	-0.32	0.09
96146	6148	87	4.12	0.11	0.12	0.10

4.2. From Model Atmospheres

In addition, we derived global atmospheric parameters with the use of model atmospheres. These computations were run for spectrograms measured at the ORO and FLWO. Here, we used one-dimensional correlations to identify the template in the library of synthetic spectra that gives the best match with the observed spectrum. We chose the template that gave the highest peak correlation value averaged over all the observed spectra for each program star. We assumed solar metallicity for all but five high proper-motion stars, namely, HIP 98655, HIP 97168, and HIP 98829, for which we used $[\text{Fe}/\text{H}] = -0.5$, and HIP 94704 and HIP 99267, for which we used $[\text{Fe}/\text{H}] = -1.5$, and then we solved for effective temperature and surface gravity. The composite spectrum of HIP 94335 was analyzed with a two-dimensional correlation technique TODCOR (Zucker & Mazeh 1994, and Torres et al. 2002). Grids of solutions were run using the CfA library of synthetic spectra as templates in order to find the individual templates for the primary and secondary that gave the best match to the observed spectra. Solar metallicity was assumed for this analysis, and surface gravities of $\log g = 4.0$ and 4.5 were adopted for the primary and secondary, respectively. The best match to the observed spectra was achieved using a template with $T_{\text{eff}} = 6060 \pm 50$ and $v \sin i = 30 \pm 2$ for the primary and $T_{\text{eff}} = 5390 \pm 250$ and $v \sin i = 24 \pm 4$ for the secondary. In Table 11, we list the parameters obtained for 14 PATS and 14 remaining stars.

The difference between effective temperature obtained with the use of ELODIE grid and the model atmospheres is plotted as a function of T_{eff} (ELODIE) in the upper right panel of Fig. 6. In most cases, the values agree to within the error bars. Only for HIP 94145, HIP 95843, HIP 98829, and HIP 99267 there are high

T a b l e 11

Astrophysical parameters of 14 PATS and 14 remaining stars determined with the use of model atmospheres
(as elsewhere in this paper HIP 94335 is counted as one star)

HIP	T_{eff}	$\log g$	[Fe/H]	HIP	T_{eff}	$\log g$	[Fe/H]
PATS				The remaining stars			
93011	6500	3.5	0.0	91128	4250	3.5	0.0
94335-1	6060	4.0	0.0	92922	5500	4.0	0.0
94335-2	5390	4.5	0.0	94145	7500	4.5	0.0
94497	5000	4.5	0.0	94704	5250	4.5	-1.5
94565	6000	3.5	0.0	94743	7000	4.0	0.0
94734	5750	4.0	0.0	94898	5250	4.0	0.0
95098	6000	3.5	0.0	95631	5250	4.0	0.0
95637	6750	4.5	0.0	95638	5750	4.5	0.0
95733	5500	4.5	0.0	95843	6750	4.5	0.0
96634	5250	4.5	0.0	96146	6250	4.0	0.0
96735	5000	4.5	0.0	97168	5500	4.5	-0.5
97219	5250	4.5	0.0	98381	4500	4.0	0.0
97657	4750	4.5	0.0	98829	5000	3.5	-0.5
97974	6000	4.5	0.0	99267	6750	5.0	-1.5
98655	5000	4.5	-0.5				

discrepancies.

For HIP 99267, T_{eff} computed from model atmospheres is 752 K higher than that obtained from ELODIE grid, which is equal to 5998 K. It is also higher than other determinations that can be found in the literature, and which range from 5650 K (Carney et al. 1997) to 5857 K (Laird et al. 1988). For HIP 94145, classified in this paper and by Macrae (1952) to F0 III, the effective temperature obtained from model atmospheres is around 400 K higher than T_{eff} derived from ELODIE grid, and is not consistent with T_{eff} expected for a typical F0 giant (see, e.g., Alonso et al. 1999). For HIP 98829, classified in this paper to G8V and by Dieckvoss & Heckmann (1975) to G5, the effective temperature obtained from model atmospheres is around 600 K lower than the one derived from ELODIE grid, and is typical for a K2V star. For HIP 95843, that is a slightly metal-deficient star classified to F2V in this paper and to F2 by Dieckvoss & Heckmann (1975), the T_{eff} derived from model atmospheres is around 500 K higher than the one derived from ELODIE grid. The source of these discrepancies is not clear. After rejecting these four stars, the mean difference between T_{eff} determined from ELODIE grid and the model atmospheres is equal to $+26 \pm 122$ K.

For $\log g$, the difference $\log g$ (ELODIE) – $\log g$ (MODEL) is shown in the right lower panel of Fig. 6. These values show good overall agreement with a mean equal to -0.02 ± 0.43 dex. The highest discrepancies occur for HIP 91128 and HIP 99267.

5. Projected Rotational Velocity

In Table 12, we list projected rotational velocities of the program stars. For each star, two values are given, one determined from a grid of Kurucz model spectra (columns headed “model”), and another, determined with the Full Width at Half Maximum (FWHM) method.

T a b l e 12
 Projected rotational velocities determined from a grid of Kurucz model spectra
 and from the FWHM method

HIP	$v \sin i$ [km s ⁻¹] (model)	$v \sin i$ [km s ⁻¹] (FWHM)	s.d. [km s ⁻¹] (FWHM)	HIP	$v \sin i$ [km s ⁻¹] (model)	$v \sin i$ [km s ⁻¹] (FWHM)	s.d. [km s ⁻¹] (FWHM)
PATS				The remaining stars			
93011	30.0	28.8	0.8	91128	1.0	<5.0	
94335-1	29.5	32.7	1.2	92922	1.5	<5.0	
94335-2	25.0	28.0	2.0	94145	12.3	14.3	1.1
94497	0.0	<5.0		94704	1.5	<5.0	
94565	7.3	7.4	1.0	94743	15.7	14.7	0.6
94734	1.5	<5.0		94898	3.0	<5.0	
95098	3.0	<5.0		95631	2.5	<5.0	
95637	28.5	29.5	0.9	95638	1.5	<5.0	
95733	0.5	<5.0		95843	12.6	17.1	1.0
96634	1.5	<5.0		96146	33.5	35.6	1.6
96735	1.5	<5.0		97168	1.5	<5.0	
97219	0.0	<5.0		98381	1.5	<5.0	
97337	—	<5.0		98829	3.0	<5.0	
97657	0.0	<5.0		99267	7.6	10.4	2.0
97974	1.5	<5.0					
98655	1.5	<5.0					

We have used the Kurucz model spectra (see Sect. 2) for stars observed with the MMT, Wyeth, and Tillinghast telescopes. In this method, each observed spectrum is compared with a library of synthetic spectra using correlation techniques described already in Sec. 4.2. A typical standard deviation of these determinations is equal to 1 or 2 km s⁻¹.

For stars observed with FRESKO, we have determined $v \sin i$ using the FWHM method for each order of the echelle spectrum. We excluded orders containing very broad spectral lines that can affect the shape of the cross-correlation function. As templates, we used a grid of rotationally broadened spectra of a non-rotating star having a similar T_{eff} , $\log g$, and [Fe/H] as the program star. An upper limit of 5 km s⁻¹ has been estimated according to the instrumental resolution of the spectrograms. The values of $v \sin i$ larger than this limit are listed in Table 12 together with their standard deviations.

As can be seen from Table 12, the values of $v \sin i$ obtained from the two separate sets of data by means of the above-mentioned two methods agree well. The only exception is HIP 99267, an extremely metal-poor star with so few lines that it was difficult to obtain a precise value of $v \sin i$ using the FWHM method.

6. Summary

We present spectroscopic observations of 15 best candidates for Kepler primary asteroseismic targets (PATS) and of 14 other program stars. The observations were carried out at the *M.G. Fracastoro* station of the Catania Astrophysical Observatory, the Oak Ridge Observatory, Harvard, Massachusetts, and the F.L. Whipple Observatory, Mount Hopkins, Arizona.

We find that all PATS have solar-like metallicity or are slightly metal-deficient. They range from early F-type to late K-type, so that we expect all of them to show solar-like oscillations. Four PATS we classify as subgiants or giants. These stars are particularly interesting from the asteroseismic point of view because the predicted amplitude of solar-like oscillations in the evolved stars is expected to be higher than in dwarfs (see, e.g., Kjeldsen & Bedding 1995).

From all spectrograms, we derive the radial velocities. The results are given in Table 2, available in electronic form from the Acta Astronomica Archive (see the cover page). The spectrograms obtained at the *M.G. Fracastoro* station of the Catania Astrophysical Observatory are used to determine the effective temperature, surface gravity, metallicity, and MK type by means of the ROTFIT code (Frasca et al. 2003, 2006). The spectrograms obtained at the Oak Ridge Observatory and the F.L. Whipple Observatory are used to determine the effective temperature and surface gravity by means of a two-dimensional correlation technique TODCOR (Zucker & Mazeh 1994 and Torres et al. 2002). The results obtained from these two different methods applied to two different data sets and given in Tables 9, 10, and 11, agree well in most cases. We also estimate the projected rotational velocity from two separate sets of data using two independent methods (see Table 12), obtaining good agreement.

We discuss in some detail three program stars that show variable radial-velocity, viz., HIP 94335, HIP 94734, and HIP 94743. For HIP 94335 = FL Lyr, one of the PATS and a well-known Algol-type eclipsing variable and a double-lined spectroscopic binary, we find close agreement between orbital elements computed from our data (see Table 4 and Fig. 1) and those of Popper et al. (1986). For this star precise determination of mass and radius exist in the literature (see Torres et al. 2006 and references therein) that can be used either as an additional constraint for pulsational modeling or as a test of its results.

HIP 94734, which is one of PATS, and HIP 94743 = V 2077 Cyg, which does not fall onto active pixels of Kepler CCDs, we have discovered to be single-lined systems. For both, we derive orbital elements (see Tables 5 and 6, and Figs. 2 and 3). In addition, using our value of the orbital period and Hipparcos epoch photometry (ESA 1977), we demonstrate that HIP 94743 = V 2077 Cyg is a detached eclipsing binary (see Fig. 4).

Our data do not confirm the spectroscopic-binary status of HIP 97219 = HD 187055, reported to be variable in radial velocity by Nordström et al. (2004), and HIP 99267 = G125-64, suspected to be a spectroscopic binary by Carney and Latham (1987).

Acknowledgments. This work was supported by MNiSW grant N203 014 31/2650, the University of Wrocław grants 2646/W/IA/06 and 2793/W/IA/07, the Italian government fellowship BWM-III-87-Włochy/ED-W/06 and the Socrates-Erasmus Program “Akcja 2” 2006-2007, contract No. 33. J.M.-Ż. thanks the Danish Natural Science Research Council, the Italian National Institute for Astrophysics (INAF), the University of Catania, and the University of Wrocław for the financial support.

We acknowledge the partial support from the Kepler mission under cooperation agreement NCC2-1390 (D.W.L., PI).

REFERENCES

Alonso, A., Arribas, S., and Martnez-Roger, C. 1999 *Astron. Astrophys. Suppl. Ser.* 140 261

- Borucki, W.J., Koch, D.G., Dunham, E.W., and Jenkins, J.M. 1997 ASP Conf. Ser. vol. 119 p.153 ed. David Soderblom
- Carney, B.W., and Latham, D.W. 1987 *Astron. J.* 93 116
- Carney, B.W., Wright, J.S., Sneden, C., Laird, J.B., Aguilar, L.A., and Latham, D.W. 1997 *Astron. J.* 114 363
- Christensen-Dalsgaard, J. 2004 *Solar Physics* 220 137
- Dieckvoss, W., and Heckmann, O. 1975 AGK3 Catalogue
- ESA 1997 "The Hipparcos and Tycho Catalogues" ESA SP-1200
- Frasca, A., Alcalà, J. M., Covino, E., Catalano, S., Marilli, E., and Paladino, R. 2003 *Astron. Astrophys.* 405 149
- Frasca, A., Guillout, P., Marilli, E., Freire Ferrero, R., Biazzo, K., and Klutsch, A. 2006 *Astron. Astrophys.* 454 301
- Johnson, H.L. 1966 *Ann. Rev. Astron. Astrophys.* 4 193
- Katz, D., Soubiran, C., Cayrel, R., Adda, M., and Cautain, R. 1998 *Astron. Astrophys.* 338 151
- Kazarovets, A.V., Samus, N.N., Durlevich, O.V., Frolov, M.S., Antipin, S.V., Kireeva, N.N., and Pastukhova, E.N. 1999 IBVS No. 4659
- Kjeldsen, H., and Bedding T. 1995 *Astron. Astrophys.* 293 87
- Laird, J.B., Carney, B.W., and Latham, D.W. 1988 *Astron. J.* 95 1843
- Latham, D.W., Mazeh, T., Stefanik, R.P., Davis, R.J., Carney, B.W., Krymolowski, Y., Laird, J.B., Torres, G., and Morse, J.A. 1992 *Astron. J.* 104 774
- Latham, D.W., Stefanik, R.P., Torres, G., Davis, R.J., Mazeh, T., Carney, B.W., Laird, J.B., and Morse, J.A. 2002 *Astron. J.* 124 1144
- Macrae, D.A. 1952 *Astrophysical J.* 116 592
- Molenda-Żakowicz, J., Arentoft, T., Kjeldsen, H., and Bonanno, A. 2006 Proc. SOHO 18/GONG 2006/HELAS I, CDROM, p. 110.1
- Nordström, B., Mayor, M., Andersen, J., Holmberg, J., Pont, F., Jørgensen, B.R., Olsen, E.H., Udry, S., and Mowlavi, N. 2004 *Astron. Astrophys.* 418 989
- Popper, D.M., Lacy, C.H., Frueh, M.L., and Turner, A.E. 1986 *Astron. J.* 91 383
- Prugniel, Ph., and Soubiran, C. 2001 *Astron. Astrophys.* 369 1048
- Soubiran, C., Katz, D., and Cayrel, R. 1998 *Astron. Astrophys. Suppl.* 133 221
- Torres, G., Boden, A.F., Latham, D.W., Pan, W., and Stefanik, R. 2002 *Astron. J.* 124 1716
- Torres, G., Lacy, C.H., Marschall, L.A., Sheets, H.A., and Mader, J.A. 2006 *Astrophys. J.* 640 1018
- Udry, S., Mayor, M., Maurice, E., Andersen, J., Imbert, M., Lindgren, H., Mermilliod, J.-C., Nordström, B., and Prévot, L. 1999 IAU Coll. 170 ASP Conf. Ser. 185 p. 383
- Zucker, S., and Mazeh, T. 1994 *Astrophys. J.* 420 806